ENGINEERING RESEARCH JOURNAL (ERJ)
Vol. 1, No. 40 April 2019, pp. 24-38.
Journal Homepage: www.feng.bu.edu.eg

Simulation of a Hybrid Solar-Wind Power Plant Using Different Nano Particles Concentrations for New Capital of Egypt Case Study

Bassam Adel[1], , M. H. Mohamed[1,2] , Mohamed Aly[1] and E.Elgendy[3]

[1] Mechanical Power Engineering Dept., Faculty of Engineering-Mattaria, Helwan University, Cairo, Egypt

[2] Mechanical Engineering Dept., College of Engineering and Islamic Architecture, Umm Al-Qura University, Makkah, Kingdom Saudi Arabia

[3] Mechanical Engineering Department, College of Engineering and Technology-Cairo Campus, Arab Academy for Science, Technology and Maritime Transport (AASTMT)

Abstract. Clean renewable energy applications grow fast due to the climatic change issue. This paper investigates two different parabolic trough solar power plants using Therminol VP-1 and solar salt as heat transfer mediums respectively for the meteorological data of the New Capital of Egypt. Both investigated power plants are based on a modified model of Nevada Solar One, which showed a design efficiency and annual average efficiency of 22.17% and 15.36%, respectively in agreement with the verification model from literature review data. Simulation results shows limited error ranges up to 3.78% using Engineering Equation Solver software with the aid of Meteonorm 7.0 weather database. The study is conducted for both power plants performance using Al_2O_3 and Cu Nano particles volumetric concentrations up to 5%. Design conditions simulation results show that using solar salt as a heat transfer fluid improves the power generation to 45.44 MW, which is 3% higher than the Therminol VP-1. Annual performance simulation results show that solar salt power plant using 5% of Cu Nano particles gives the best performance among all of the investigated cases. Solar salt power plant using 5% of Cu Nano particles produces 103 GWh net annual power generation and average annual efficiency of 25.02%. Finally the performance of the best case scenario is investigated using the hybrid solar-wind power generation. Wind energy generation is found to produce net output energy of 1.56 GWh annually using a proposed wind turbine model from literature data.

Keywords: Parabolic Trough; Nano particles; Hybrid system; HTF.

Nomenclature

- **Symbols**

δ	Declination	C_p	specific heat (J/Kg.°K)
$\emptyset$	latitude angle	**T**	temperature (°K)
α	Absorptivity	ΔP	pressure difference (Pa)
η	Efficiency	ξ_{EV}	focal length losses
θ	incidence angle	ξ_{IAM}	incidence losses
ξ	shadow losses	ξ_{shadow}	shadow losses
ρ	density (Kg/m^3)	$Q^{\bullet}_{SF}$	solar field heat gain (Watt)
τ	transmissivity	$m^{\bullet}_{HTF}$	mass flow rate of HTF (Kg/s)
Φ	concentration ratio	P_{wind}	wind Power (Watt)
ω	hour angle	$W^{\bullet}$	work rate (Watt)
N	day Number	θ_z	zenith angle
y	mass fraction	**h**	enthalpy (J/Kg)
ρ_{mir}	mirror reflectivity	$C_{p,w}$	betz coefficient
`L	trough length	L_f	focal length (m)
P	power (Watt)	**E**	power (Watt)

- **Acronyms**

LPT	low pressure turbine	**ACS**	active construction center
HPT	high pressure turbine	**SNL**	sandia national laboratory
IPCC	intergovernmental panel on climate change	**FVM**	finite volume method
		Ppm	part per million
ORC	organic Rankine cycle	**MCRT**	Monte Carlo Ray-Trace
LCOE	levelized cost of energy	**SM**	solar multiple
PV	photo-voltaic	**HAWT**	horizontal axis wind turbine
DNI	direct normal irradiation	**VAWT**	vertical axis wind turbine
CSP	concentrated solar power plants	**MWCNT**	multi-walled carbon nano
PTC	parabolic trough collector	**HITEC**	$NaNO_3 - NaNO_2 - KNO_3$
DSG	direct steam generation	**HITEC XL**	modified HITEC
HTF	heat transfer fluid	**DUKE**	Durchlaufkonzept Entwicklung und Erprobung
TES	thermal energy storage	**APROS**	simulation tool
EES	engineering equation Solver	**AZTRAK**	rotation platform at SNL
ASPEN	simulation tool		

- **Subscripts**

amb	Ambient	***temp***	temperature
Elec	electrical	***F***	base fluid
s f	solar field	***Conc***	concentration
HTF	Fluid	***Th***	thermal
Rec	Receiver	***nf***	nano-fluid
Over	Overall	**ss**	solar salt
IAM	incidence angle modifier	**Isen**	Isentropic

1. INTRODUCTION

The anthropogenic greenhouse gas concentration and global average of temperature were recorded by the IPCC 2007 [1] to reach their peak value with a dramatic increase to about 390 ppm (39% increase compared to the pre-industrial records and 0.76℃ increase in Earth's average of temperature. Many international organizations predicted that the current levels of CO_2 emissions would lead into 2℃ increase of earth's temperature [1] and about 450 ppm for CO_2 emission. UN members signed the Climate Change Agreement in Paris 2015 [2] to maintain the temperature of the earth and CO_2 emissions within their acceptable level. Earth receives about 1.8×10^{11} GW of energy from the sun. Therefore, the current demand from the world's energy is about only 1% of this amount [3]. Clean renewable energy resources are the main scope of most power generation studies with their different application.

Powell et. al. [4] reviewed most commonly used hybrid solar energy systems implemented worldwide or suggested by researchers using bio-mass, fuel fired back up, ORC and wind energy. They showed their advantages based on efficiency, economy, reliability and LCOE in a comparative study. Al-Falahi et. al. [5] reviewed the most modern applied system for rural areas and location; in addition to reviewing the modern trends in software tools used to predict their performance. PV-Wind-Diesel hybrid back-up system was found to be the most frequent choice for this application based on metrological and economic factors, load profile, reliability and even social interface. S. Dihrab and K. Sopian [6] developed a mathematical model to predict the monthly average power generation over three different locations in Iraq by a PV-wind hybrid System. The DNI was found to be the most effective parameter that contributes to higher power generation.

In this paper, the main study is solar energy production using PTC which is shaped in the form of parabolic glass mirror and a focal line positioned at a long tube absorber. This technology could be used in DSG to produce Steam directly S. Ravelli et. al [7] and then the parabolic trough collector solar field, is considered to be Rankine cycle boiler as implemented in Almeria power plant. Mario Biencinto et. al. [8] also investigated the performance of PTC mathematical model using TRNSYS with two different modes of controlling the steam pressure of a DSG 38.5 MW power plant concluding that the variable pressure regulation strategy is more efficient through the entire power generation process.

The CSP technology uses a heat transfer fluid which have specific technical thermo-physical properties, such as Therminol VP-1 and other Therminol types, Sylthrem 800 and Dowtherm A. The heat absorbed by the solar field transfers to the HTF which exchanges heat with the steam used to run the Rankine cycle. A part of energy can be stored in a TES to supply heat to the power plant during the night time hours or cloudy periods. Zarza et. al. [9] developed a mathematical model to investigate the performance of Sevilla 5 MW DSG power plant. The study concluded that system optimized operational temperature is about (260 ~ 300°C) from the cost point of view. Feldhoff et. al [10] investigated the new PTC technologies during the DUKE project. The new collectors were designed to have better optical efficiency about 77% and showed low rates of heat losses which led to larger energy supply into the power block as well.

F. Trieb et. al. [11] developed a simulation code using EES to simulate the performance of many implemented solar power plants in different locations with different PTC types, LS-2, LS-3 and Fresnel using EES mathematical model for different PTC and power. They investigated the performance of each PTC solar power plant for different condenser cooling methods. They proposed a simplified equivalent schematic layout for each power plant for different meteorological data through the simulation procedure. I. L. Garcia et. al. [12] investigated the performance of 50 MW Andasol power plant which is equipped by a TES to supply heat during night hours. The simulation was carried out to study the instantaneous performance of the power plant using EES and the true data supplied by ACS. Y. Li, Y. Yang investigated the coexistence of TES using ASPEN plus model through different solar multiple (SM) ranges varied from (1.1 ~ 1.5). They concluded that increasing the SM factor will increase the power generation, however the LCOE will increase as well. The results showed that the best-case scenario to be (SM = 1.2) [13] from the Thermo-economic point of view. W. Al-Maliki et. al [14] investigated the performance of 50 MW Andasol solar power plant and compared the simulation data with the recorded data by operator with acceptable range of errors for the simulation data conducted by APROS software.

The heat transfer fluid (solar field fluid) has a significant influence on the performance of the solar power plant since the thermo-physical properties and the fluid chemical composition are the major affecting parameters through the calculation of the pumping power, hydraulic losses and the thermal model of the solar power plant [15]. S. A. Kalogirou [16] developed an EES code to simulate the thermal circuit of the parabolic through absorber for steady state conditions with different sets of modeling equations the research concluded that one dimensional model is simple and provides acceptable range of errors during the study of plant performance compared to the 3D thermal circuit model.

E. Bellos et. al [17] discussed the performance of an EU-150 PTC using 7 different fluids which are pressurized water, Therminol VP-1, nitrate molten salt (Known as basic binary solar salt), Sodium liquid, air, CO_2 and Helium under temperature ranges of (300 ~ 1300 °K). Results showed that water gives the better performance for temperature ranges lower than 550°K and CO_2 is the best solution for temperatures ranges over 1100°K ; whereas the liquid sodium shows the highest range of exegetic performance. Z.D. Cheng et. al. [18] investigated the effect of different HTF over LS- PTC used in AZTRAK operated by SNL using FVM and MCRT methods; they concluded that Therminol and Sylthrem 800 have better thermal performance over HITEC XL and solar salt from the first law of thermodynamics analysis point of view. D. Bishoyi and K. Sudhakar [19] suggested a PTC solar power plant using HITEC as a HTF for an output power of 100 MW in Rajastan, India. Simulation results showed that the overall solar-to-electric efficiency could reach to 21% and 285 GWh of output electrical power.

The HTF thermo-physical properties can be modified using small concentrations of Nano-particles. Similar to the applications implemented widely in many industries of metal alloying, refrigeration, lubricants and oil. Nano particles offer a smart way to change the thermo-physical properties of the medium. Many researchers discussed the effect of using Nano-particles additives through the solar power plant thermal performance. Colongelo et. al. [20] investigated experimentally the effect of Cu, CuO, ZnO and Al_2O_3 Nano particles on the behavior of thermal conductivity of the Diathermic oil. Results showed that ZnO increases the thermal conductivity more than other Nano particles. A Kasaeian et. al. [21] developed an experimental test rig called the pilot through collector (0.7m width) using different concentrations of MWCNT. Results showed that 0.2% addition of MWCNT leaded into increasing system thermal efficiency by (4-5) % whereas 0.3% addition increased the system thermal efficiency to (5-7%).

V. Ferrero et. al. [22] investigated the performance of PTC using Synthetic oil as a HTF with different concentrations of Al_2O_3 Nano particles which resulted into slightly increase in power generation but leaded into increasing the parasitic pumping power as well. E. Bellos and T. Christos [23] developed a mathematical model to investigate the power generation performance for EU-150 PTC using Sylthrem 800 as a HTF by the addition of Al_2O_3 and CuO Nano particles; the study concluded that both options leaded into increasing the system thermal efficiency. Chan Z. et. al. [24] also investigated the thermal conductivity of Diathermic oil based on SiC Nano particles. Results showed that 0.8% addition of SiC Nano particle would increase the thermal conductivity by 7.36% but for lower concentrations the effect is slightly lean.

Many researchers investigated the simulation of different PTC models using different simulation tools and different mathematical models. Heat transfer fluids play an important role in the solar field performance since a slight variation in their thermo-physical properties results in significantly large change in the thermal model of the solar field. The Nano particles contribute into changing the thermo-physical properties of the heat transfer fluid without changing their chemical composition to enhance the thermal performance of the PTC power plant. The present work investigates two different PTC technologies to allow the use of two different HTF with widely changing temperature ranges. Then the case of pure HTF is compared to the addition of different Nano particles concentrations. Finally based on the best-case scenario the hybrid wind-solar power generation system is investigated to compare those cases with the basic pure Therminol VP-1 stand-alone power plant. The study uses EES mathematical model to predict the design point, annual and monthly performance.

2. MATHEMATICAL MODEL

Hybrid solar-wind power generation performance majorly depends on the meteorological data of the proposed location. In this paper, Nevada Solar-One lay out power plant is chosen to be the basic case of study and verification model as well [25]. The solar power plant operational input parameters, steam conditions and assumptions used to simulate the performance of the power plant obtained by A. Giostri et. al. [26] are listed in Table [1]. Nevada Solar-One is a 75 MWe power plant uses Therminol VP-1 as a HTF using EU-100 as a PTC model since Therminol VP-1 maximum operational temperature is limited to 400 °C [25] . Solar salt can operate under temperature levels up to 600 °C as elaborated in the next section of the paper so it uses HEMS08 as a PTC. HEMS08 PTC is implemented in Archimede solar power plant [27] which produces 5 MWe of electric output power. It uses solar salt as a HTF located in Italy. Fig. (1) shows a schematic layout of the proposed power plant. Fig. (1) also indicates the investigated parameters in the present work which are the use of Nano particles, solar salt as a HTF and the aid of wind power generation respectively under Nevada and New Capital meteorological data respectively.

TABLE 1. Design parameters for investigated power block

HPT isentropic efficiency	85%
LPT isentropic efficiency	88%
Feed water pump hydraulic efficiency	75%
Condensate pump hydraulic efficiency	70%
Pump mechanical – electrical efficiency	94%
Boiler thermal losses	1.5%
Temperature difference in Feed water	3°C
Air temperature increase	10°C
Condenser gauge pressure	0.096 bar
Fan efficiency	75%
Heat exchanger loss	1.5%
Proposed Locations	New Capital and LV, Nevada
Generator efficiency	97%

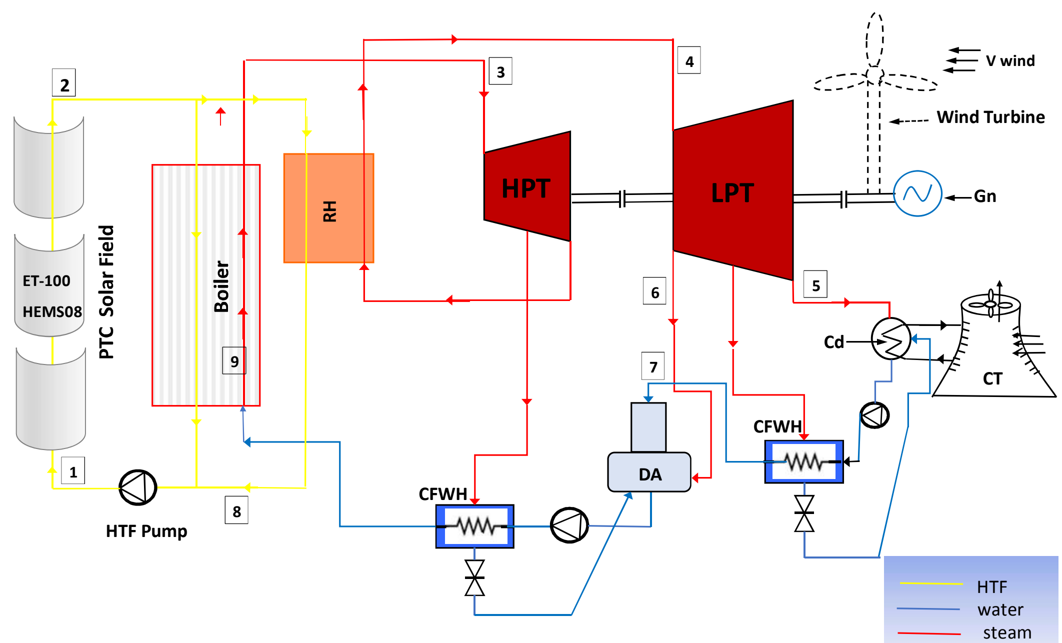

CFWH	Closed Feed Water Heater	**HPT**	High Pressure Turbine
DA	Deaerator	**LPT**	Low Pressure Turbine
RH	Reheater	**CT**	Cooling Tower
Cd	Condenser	**Gn**	Generator

FIGURE 1. Investigated Hybrid PTC-Wind Power Plant

2.1 System Components

In this section, the input data, mathematical equations, assumption of every single component of the power plant, HTF properties as well as Nano particles properties will be discussed and elaborated. The solar radiation, coming from the sun, is absorbed by the PTC field using different types of tracking systems to maximize the useful thermal energy transferred to the PTC or to minimize the fluctuations in the output power profile. In this study the single axis tracking system in north south axis of orientation is chosen as it maximize the heat gained by the PTC regardless the fluctuations in the produced performance profile [12]. Two PTC models are chosen to meet the various ranges of the operating temperatures of the different HTF used in the simulation process as follows:

- ET-100 PTC with maximum operating temperature of 400°C [28].
- HEMS08 PTC with maximum operating temperature of 600°C [27].

The following Table [2] shows the main geometrical and optical specifications for each PTC besides the major operating conditions of solar salt and Therminol VP-1. The table also summarizes general data about both PTC power plants and their solar fields.

TABLE 2. PTC geometrical and optical properties, HTF general data and solar

	Component	**ET-100**	**HEMS08**
PTC Model	-Receiver	SOLEL [28]	HEMS08 [26]
	-Mirror	FLABEG	HEMS08
Geometrical Properties	-Focal length	1.71 m	1.81 m
	-Aperture width	5.77 m	6 m
	-Collector length	99.5 m	100 m
	-Aperture Area	545 m^2	590 m^2
Optical Properties	-Reflectivity	94%	94%
	-Absorbance	96%	95~96%
	-Transmissivity	97%	99%
	-emissivity	14~16%	13~16%
Operating condition	-Basic HTF	Therminol VP-1	Solar salt (Binary)
	-HTF Temperature Ranges	$T_{in} = 290°C$ $T_{out} = 390°C$	$T_{in} = 290°C$ $T_{out} = 550°C$
	-Crystallization Point	12 °C [28]	220°C [27]
	-Temperature range	12~400 °C	220~600°C
	-Chemical Composition	Biphenyl/Diphenyl Oxide-Eutectic mixture	60%$NaNO_3$ + 40% KNO_3 Binary mixture
General Data	-Plant Name	Nevada solar one	Archimedes power plant
	-Plant Location	USA	Italy
	-Gross power	75 MW	5 MW

The simulation mathematical model for both cases is investigated for the New Capital of Egypt meteorological data conditions. The following Table [3] shows a sample of Meteorological data obtained from Meteonorm 7.0 [29] weather data base.

TABLE 3. Meteorological data for the proposed locations

Name	**New Capital**
Location	Egypt
Latitude	30° 1′ 48″ North
Longitude	31° 46′ 48″ East
Annual DNI	2116 kW.hr/m² per year [**29**]
Average wind speed	3.55 m/sec

To simplify the simulation procedure and ensure that output results only depend on the investigated parameters the following operating conditions and assumptions are set to be constant during the simulation process:

- Solar DNI generates heat supply to heat up the HTF used in both cases within the required range to operate the power block as follows through the simulation code where the maximum available heat from the sun is calculated from equation (1); [10] regardless the fluctuations in the solar DNI

$$E_{sun} = DNI\ A_{apperture} \quad (1)$$

- Basic simulation code assumes constant temperature ranges during the steady state operation within the operating range of temperatures listed in Table [2] for both HTF.
- Thermal properties of the HTF basic fluids are then influenced by the addition of Al_2O_3 and Cu Nano particles using volumetric concentrations up to 5% with constant densities of 3850 kg/m³ and 8933 kg/m³ for Al_2O_3 and Cu Nano particles respectively obtained by [30] and [31].

- As the heat transfer rate supplied to thermal power block increases the amount of heat supplied to the boiler increases as well. It results in increasing steam evaporation and production process resulting in larger power generation due to high specific enthalpy through turbine inlet but within the maximum temperature ranges listed in Table [2].
- The power block system is based on regenerative reheat Rankine cycle as shown in Fig. (1). The boiler is divided into three major parts which are economizer, evaporator and superheater respectively and the reheat process takes place only in the third stage of boiler process to ensure that both turbines input temperatures are at the maximum operating design temperatures 370°C for Therminol VP-1 and 540°C for solar salt.
- The steam turbine model is Siemens 700/900 ST series [32] which can work up to 165 bar and 565°C inlet condition to provide the sufficient temperature ranges required for each HTF.

2.2 Simulation Procedure

Both PTC power plants are set to produce 50MW of electric power within the two basic cases to ensure that the comparison through this study only depends on the investigated parameters regardless solar field area, layout design and cost analysis. To set both power plants to produce 50 MWe output power the mass flow rates for HTF and the produced steam are recalculated according to Gistori et. al. [26] and [33]. Table [4] simplifies the operational thermodynamic state for each point of the power block besides the HTF mass flow rates and operational temperature ranges. Both modified mathematical models for the new operational conditions of Nevada Solar-One and Archimede power plants is verified with Gistori et. al. [26] as discussed later in this paper. The mathematical model is conducted for the meteorological data of the New Capital for both PTC models using the investigated two HTF with the different concentrations of Al_2O_3 and Cu Nano particles. Finally the best case scenario of those investigated cases is compared with the hybrid solar-wind power generation [6] and [3٤].

TABLE 4. Thermodynamic properties for each state of the system

Point	Fluid	Therminol VP-1			Solar Salt		
		$m^{\bullet}_{HTF}$	p	T	$m^{\bullet}_{HTF}$	p	T
		(Kg/s)	(bar)	(°C)	(Kg/s)	(bar)	(°C)
1	HTF	725.8	25	308	355.9	15	312.7
2	HTF	618.7	17.6	390	296.6	3.7	550.0
3	Steam	63.5	95	370	47.1	115	540.0
4	Steam	51.6	14.5	370	37.9	14.5	45.0
5	Steam	49.1	0.096	45	30.8	0.096	45.0
6	Steam	2.6	9.2	312.8	1.6	9.2	471.4
7	Water	49.1	8.7	143.9	36.3	8.7	143.9
8	Water	63.5	117.6	260.4	47.1	141.2	278.9
9	Water	63.5	100	299.5	47.1	120	313.4

The following Fig. (2) shows the simulation procedure flow chart process used to estimate the design point, annual performance and monthly performance of the proposed solar power plant. Simulation procedure starts by identification of the meteorological data inputs, location, power block thermal model, HTF properties and Nano particles properties. The corresponding geometrical and thermal losses are used to estimate the net output power generation. Through the simulation process, the solid lines represent the reference investigated pure Therminol VP-1 power plant for the New Capital meteorological data. The dashed lines represent the investigated parameters through this paper for the New Capital meteorological data.

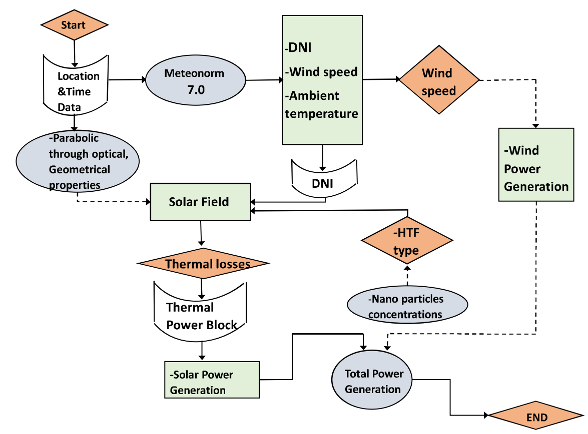

FIGURE 2. Simulation program process

2.3 Mathematical Model

The mathematical model divides the system components into four major parts. The first part is the solar field which consists of PTC model and HTF recirculation pump. Two PTC are investigated to achieve the required operational temperature ranges of the two HTF. The second part is a counter flow heat exchanger in which thermal energy of the HTF is exchanged with the thermal energy of the steam of Rankine cycle. The steam evaporation process takes place only in the third stage of this part of the system due to the assumption listed in section (2.1). The third part is a reheat regenerative Rankine cycle. The Rankine cycle is responsible for converting the thermal heat of the steam into output rotational mechanical work to produce electricity in the electrical generator. The fourth part is the wind power generation using the proposed wind turbine regardless the wind to CSP ratio of the proposed location.

2.3.1 Sun collector Geometry

The following set of equations are used to obtain the useful effective component of the DNI which produces heat through the absorber tube surface to heat up the HTF .The used set of equations are obtained from [35], [36] and [7]. The day number in the year influences the declination angle due to earth's rotation around the sun as follows

$$\delta = 23.45 \sin\left(360 \times \frac{(284+n)}{365}\right) \quad (2)$$

The hour angle represents the angular displacement of the Sun=Earth system due to rotation of Earth 15°/hr. around its own axis as follows

$$\omega = 15° \times (Solar_{Time} - 12) \quad (3)$$

Those angles are used to determine the zenith angle which represents the horizontal component of the sun's beam radiation

$$\cos\theta_z = (\cos\emptyset \cos\delta \cos\omega + \sin\emptyset \sin\delta) \quad (4)$$

Where $(\emptyset)$ represents the latitude angle. Finally those sets of equations are used to determine the most important angle that influences the solar field performance mostly which is the incidence angle [14].

$$\cos\theta = \sqrt{\cos^2\theta_z + \cos^2\delta\ \sin^2\omega} \quad (5)$$

This equation is valid only for the North-South tracking system which is implemented in the present work.

2.3.2 Optical and Geometrical profile

The optical losses accompanied with the mirror optical properties are listed in Table [2]. The mirror optical properties are used to calculate the trough optical efficiency as well as the geometrical losses follows [33], [11] and [10].

$$\eta_{optical} = \alpha_{abs.} \rho_{mir}\, \tau_H\, {\tau_s}^2 \quad (6)$$

The focal length losses that occurs due to the non-exact perpendicular DNI falling on the collector are given by

$$\xi_{EV} = 1 - \frac{L_f}{L} \quad (7)$$

The incidence angle modifier is given by

$$\xi_{IAM} = \cos(\theta) - 5.251 \times 10^{-4}\theta - 2.8596 \times 10^{-5}\theta^2 \quad (8)$$

The reflection of a collector row onto the next row during the $tracking$ orientation will appear only during the early morning hours and evening hours as following

$$\xi_{shadow} = max\left[0, min\left(\frac{L}{W} \times \frac{\cos\theta_z}{\cos\theta}; 1\right)\right] \quad (9)$$

So ξ_{shadow} values are always between 0:1.

Finally those geometrical parameters are combined to produce the useful part of DNI called IDR obtained by the following equation [11] and [36]

$$\mathrm{IDR} = \eta_{optical}\, \xi_{shadow}\, \xi_{EV}\, \xi_{IAM}\ \mathrm{DNI} \quad (10)$$

Theoretical available effective heat absorbed by the absorber tube surface is given by

$$\mathrm{E_{rec.}} = \mathrm{IDR\ A_{apperture}} \quad (11)$$

2.3.3 Power Block and Heat Exchanger

Heat supplied through the solar field HTF is calculated by the following equation

$$Q^{\bullet}_{SF} = m^{\bullet}_{HTF}\, C_{p_{HTF}} \Delta T_{HTF} \quad (12)$$

The temperature difference across the HTF pump is obtained from Table [4]. The specific heat capacities of Therminol VP-1 [28] and solar salt [37] HTF are obtained from equations (1٣) and (1٤) respectively.

$$C_{P_{Therminol}} = 1.708\,T + 1107.798 \quad (13)$$

$$C_{P_{solar\ salt}} = 0.172\,T + 1396 \quad (١٤)$$

The Nano particles specific heat capacities are obtained by the following equations (1٥) and (1٦) respectively. Those equations are obtained from [37] and [38] for both investigated Nano particles

$$C_{P_{Al_2O_3}} = 1.046 + 1.74 \times 10^{-4}\,T - 2.79 \times 10^4\,T^{-2} \quad (15)$$

$$C_{P_{Cu}} = 3162.21 + 0.3177\,T - 3.4936 \times 10^{-4}\,T^2 + 1.667 \times 10^{-7}\,T^3 \quad (16)$$

While the Nano fluid mixture specific heat capacity is calculated by the following equation obtained from [38] and [39]

$$C_{P_{nf}} = C_{P_f}(1 - \Phi) + C_{P_{nP}}\,\Phi \quad (17)$$

The HTF base fluid densities are obtained by equations (١8) and (19) for Therminol VP-1 and solar salt respectively. Those equations are obtained from [28] and [37] for Therminol VP-1 and solar salt respectively

$$\rho_{Therminol} = 09079T + 0.0007T^2 - 2.36 \times 10^{-6}T^3 + 1083.25 \quad (18)$$

$$\rho_{soalr\ salt} = 2263.6 - 0.636T \quad (19)$$

The Nano fluid density [22] is obtained by the following equation

$$\rho_{nf} = \rho_f(1 - \Phi) + \rho_{np}\,\Phi \quad (20)$$

Then the PTC solar field thermal efficiency is calculated for each case by the following equation [3]

$$\eta_{thermal} = \frac{Q^{\bullet}_{HTF}}{E_{rec}} \quad (٢١)$$

The thermal heat gained by the HTF transfers to the steam through the counter flow heat exchanger to drive the Rankine cycle power block. The absorbed heat maintain the thermal energy required to approach the turbine inlet temperature listed in Table [٢]. Then the following set of equations is used to simulate the performance of the Rankine cycle based on first law of thermodynamic analysis for the proposed power plant layout as shown in Fig. (1). The thermodynamic properties of each state are listed in Table [4].

$$\eta_{H.E} = \frac{Q^{\bullet}_{Boiller}}{Q^{\bullet}_{HTF}} \quad (٢2)$$

$$\eta_{Pb} = \frac{P_{Gen}}{Q^{\bullet}_{Boiller}} \quad (٢3)$$

$$\eta_{overall} = \frac{P_{net}}{\mathrm{E_{sun}}} \quad (٢4)$$

Where the net output power which is the effective useful part of the produced electrical energy

$$P_{net} = P_{Gross} - P_{parasitics} \quad (25)$$

The parasitic load is the sum of the power lost in Rankine's power block used to drive the feed water recirculation pump, the condenser demand, cooling tower fan and the solar field pumping power dissipated in to the HTF recirculating pump. The following set of equations is used to determine net output produced power by the power block turbine and the heat dissipated in the boiler and reheater.

Boiler supplies heat input to the Rankine cycle as following:

$$Q^{\bullet}_{Boiler} = m^{\bullet}_3(h_3 - h_8) \quad (26)$$

Steam turbine output thermal power for HPT and LPT respectively are calculated as following:

$$W^{\bullet}_{HPT} = m^{\bullet}_3(h_3 - h_4) - y_1 h_{y_1} \quad (27)$$

$$W^{\bullet}_{LPT} = m^{\bullet}_4(h_4 - h_5) - m^{\bullet}_6 h_6 - y_2 h_{y_2} \quad (28)$$

Where y represents the bleeded steam mass fraction in the regenerative process.

Then the actual output power is calculated according to each turbine isentropic efficiency as following:

$$\eta_{isen,turbine} = \frac{W^{\bullet}_{actual}}{W^{\bullet}_{ideal}} \quad (29)$$

Heat supplied to the reheating process is calculated as following:

$$Q^{\bullet}_{RH.} = m^{\bullet}_4\left(h_4 - \grave{h_3}\right) \quad (30)$$

Circulation pump ideal and actual input power are calculated as following:

$$P_{pump} = m^{\bullet}_{st}\, \upsilon\ \Delta p \quad (31)$$

$$\eta_{isen,pump} = \frac{W^{\bullet}_{Ideal}}{W^{\bullet}_{actual}} \quad (32)$$

In the previous set of equations (h) is the enthalpy, (υ) is the specific volume and $(m^{\bullet}_{st})$ is the mass flow rate of steam through the cycle.

2.3.4 Wind Power Generation

The main principle of wind power generation is based on the motion of air which takes place due to the different densities of air layers due to their different temperatures through the atmosphere. There are two major types of wind turbines which are VAWT and HAWT. There are many different models of both types used for different velocity ranges within the proposed location. Both technologies depend on the energy conversion principle from kinetic energy carried by the air into mechanical energy to rotate the turbine shaft which produces electrical energy through a generator. There are several mathematical models used to predict the output power generation and torque properties. Simplest mathematical model to used obtain the output power generation by a wind turbine is Betz model [40] and [41]. This model gives the maximum theoretical power generation limit can be extracted by any wind turbine as shown in equation (33).

$$P_{wind} = \frac{1}{2}\, \rho\, C_{p,B} u^3 \quad (33)$$

$C_{p,B}$ is the Betz power coefficient which equals to 0.593. The verified model uses equation (34) to calculate the wind power generation. The technical characteristics of the wind turbine used in the simulation are given in Table [5].

$$P_{wind} = \frac{1}{2}\rho\alpha u^3 \quad (34)$$

TABLE 5. Proposed wind turbine characteristics data

Diameter (m)	Rated Power (kW)	Rated speed (m/s)
7	10	13

2.4 Mathematical Model Verification

Model verification code consists of two major mathematical models which are solar and wind power generation models respectively. Solar power generation mathematical model is verified with Gistori et. al. [26] for Nevada Solar-One modified PTC power plant as shown in in the following verification Table [6]. The verification code is conducted to calculate the design and annual performance respectively based on the meteorological data of Las Vegas location. The incidence angle and its corresponding incidence angle modifier are calculated to obtain the geometrical losses. The optical efficiency of the ET-100 is calculated for the proposed operational conditions then the effective part of the DNI is then calculated. The thermal heat supplied to the power block is then calculated based on the operational conditions of the heat exchanger and conducted for constant inlet and output HTF temperatures. Finally the performance of the power block is determined using the previous set of equations to determine the net output power and system efficiency.

TABLE 6. Solar power generation model verification table

Annual Performance Therminol VP-1 Verification Table			
Item	**Model**	**Simulation**	**Error %**
Available solar Energy MWh	722875	722875	0
Effective DNI kW.hr/m² per year	1961	1962	0.05
Receiver Solar Energy MWh	406841	406979	0.03
Thermal Energy to HTF MWh	354098	355104	0.28
Power block thermal Power MWh	344487	346489	0.58
Net Output electric energy MWh	110903	111013	0.1
Optical Efficiency	56.3	56.3	0
thermal efficiency %	87	87.25	0.29
pipe efficiency %	97.3	97.57	0.28
power block annual efficiency %	33.3	32.04	3.78
Annual overall efficiency %	15.3	15.36	0.39
Design point gross output power MW	53.2	53	0.38
Design point net output power MW	50	49.6	0.8
Design point overall efficiency %	22.4	22.17	0.34

Wind power generation mathematical model is verified with Selwan et. al [6]. The verification mathematical code is conducted for Al-Basrah, Iraq monthly average meteorological data using the wind turbine model with the characteristic data listed in Table [5]. The verification code is conducted for the monthly basis of estimation using Meteonorm 7.0 weather data base for Al-Basrah location.

TABLE 7. Wind power generation model verification

Monthly Power Generation (MWh)	Model	Simulation	Error %
January	26	25.82	0.68
February	23	22.80	0.87
March	64	64.38	0.59
April	26	25.82	0.68
May	64	64.38	0.59
June	117	114.76	1.92
July	105	104.44	0.54
August	76	75.60	0.53
September	42	41.31	1.65
October	43	43.87	2.03
November	25	24.53	1.87
December	9	8.67	3.71

3. RESULTS AND DISCUSSION

In the next section the simulation procedure discussed in Fig. (2) is carried out using Engineering Equation Solver (EES). The meteorological data of New Capital of Egypt is obtained by Meteonorm 7.0 weather database. The geometrical properties of both PTC models listed in Table [2] are then used to calculate the optical efficiency of the parabolic trough collector. Both geometrical properties, solar time and geographic location are used to obtain the effective part of the DNI and the corresponding incidence angle. Solar gain and thermal losses for Therminol VP-1 and solar salt using different Nano particles concentrations are then calculated for the solar field and the corresponding useful thermal energy is supplied to the power block. The useful thermal output power produced block is finally calculated based on the data listed in Table [4] for each HTF with different Nano particles concentration to indicate the system performance for each case. Based on the best case scenario the wind power generation is calculated using the wind turbine characteristic data listed in Table [5] to determine the corresponding wind power generation for this case.

3.1 Design point simulation results

The simulation program is firstly conducted for a 50 MW modified model of Nevada Solar One which uses Therminol as a HTF for the meteorological data for the design point obtained by National Renewable Energy Laboratory. The simulation program is carried out firstly at those design conditions and verified with the published data as shown in Table [6]. Then the simulation procedure is carried out for Therminol VP-1 and solar salt as HTF using different concentrations of Nano particles for the meteorological data of the New Capital of Egypt.

Results show that the net output power of the pure Therminol VP-1 is estimated to be 44.62 MWe at the design point conditions, whereas replacing the HTF by solar salt leads into generating 45.44 MWe net output power which is 3% greater than Therminol VP-1 as shown in Fig. (3). The using of Nano particles over both HTF leaded into enhancing the thermal properties of both HTF that results in increasing of the net output power. The Cu Nano particles were found to have better improvement on the PTC thermal performance and hence on the net output power generation. Therminol VP-1 power plant using 5% Al_2O_3 Nano particles produces 46.42 MWe; whereas Therminol VP-1 and 5% Cu Nano particles produces 46.83 MWe which is 5% higher than the pure Therminol case. Solar salt power plant using 5% Al_2O_3 Nano particles produces 47.72 MWe; whereas solar salt using 5% Cu Nano particles produces 48.17 MWe which is 5.7 % higher than the pure solar salt case.

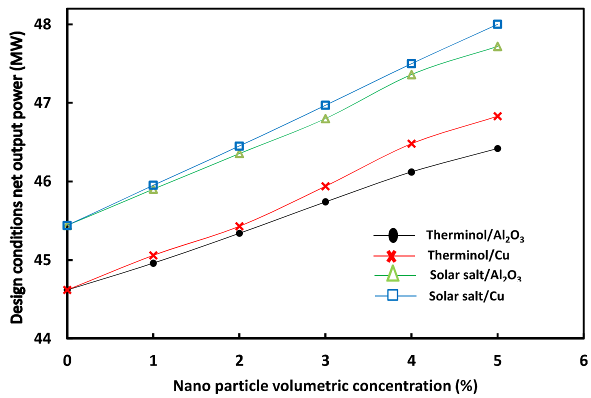

FIGURE 3. Net output power at design conditions for Therminol VP-1 and solar salt Nano fluids

The overall electric to solar efficiency depends on the net output power and the input solar gain power. The design condition assumes constant values of all the meteorological data for the investigated location, so the solar gain input power will be constant through the calculation of the net efficiency of the system. Due to the increase in the net output power produced by the solar slat field as discussed in Fig (3); the overall electric to solar efficiency increases as well by replacing the Therminol VP-1 HTF by solar salt. Pure Therminol VP-1 power plant is found have 22.17% overall efficiency whereas basic solar salt field efficiency is found to be 23.56% which is 6.3% higher than Therminol VP-1 case as shown in Fig. (4). Similar to the net output profile shown in Fig. (3) using Cu Nano particles is found to have better improve on the system efficiency. Therminol VP-1 power plant using 5% Al_2O_3 Nano particles has 22.88% overall system efficiency; whereas it is found to be 23.12% using Therminol VP-1 and 5% Cu Nano particles which is 4.2% higher than the pure Therminol case. Solar salt power plant using 5% Al_2O_3 Nano particles has 24.85% overall system efficiency; whereas it is found to be 25.02% using solar salt and 5% Cu Nano particles which is 6.2% higher than the pure solar salt case as summarized in the following Fig. (4).

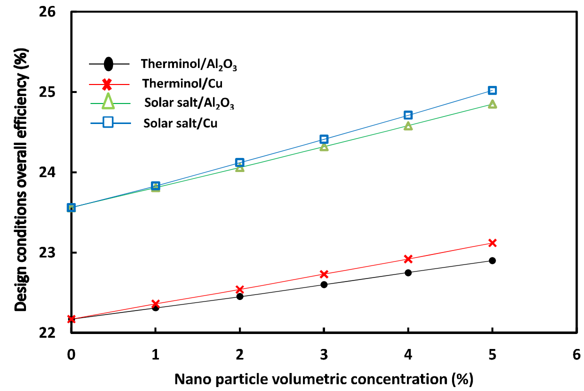

FIGURE 4. Electric-to-solar overall efficiency at design conditions for Therminol VP-1 and solar salt Nano fluids

3.2 Annual Performance simulation results

Similar to the design conditions simulation procedure the simulation program is firstly conducted for a the modified model of Nevada Solar One and then is carried out for Therminol VP-1 and solar salt as HTF using different concentrations of Nano particles for the meteorological data of the New Capital of Egypt. Results show that the net annual produced solar energy of the pure Therminol VP-1 is estimated to be 95.42 GWh, whereas replacing the HTF by solar salt leads into generating 97.52 GWh of energy which is 2.2% greater than Therminol VP-1 case as shown in Fig. (5). The using of Nano particles over both HTF leaded into enhancing the thermal performance of the proposed investigated power plant that results in increasing of the net output power as discussed in section (3.1). The Cu Nano particles are found to have better enhancement on the PTC thermal performance and hence on the net output power generation. Therminol VP-1 power plant using 5% Al_2O_3 Nano particles is found to produce 99.33 GWh; whereas Therminol VP-1 and 5% Cu Nano particles produces 100.1 GWh of annual solar energy. Solar salt power plant using 5% Al_2O_3 Nano particles produces 102.4 GWh; whereas solar salt using 5% Cu Nano particles produces 103.05 GWh which is 5.8% higher than the pure solar salt case.

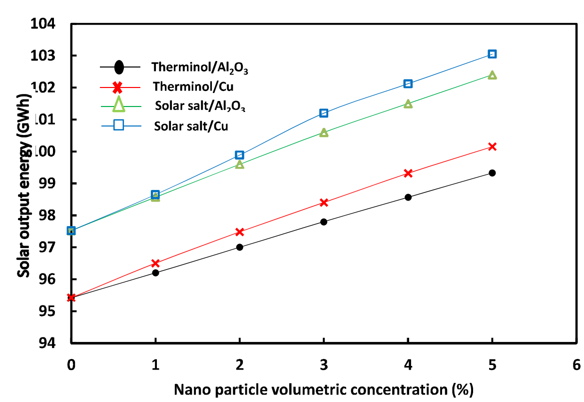

FIGURE 5. Annual net output solar energy for Therminol VP-1 and solar salt Nano fluids

The annual overall solar to electric efficiency of the pure Therminol VP-1 is found to be 15.35%, whereas replacing the HTF by solar salt leads into increasing the efficiency to 16.18% as shown in Fig. (6). The Cu Nano particles are found to have better enhancement on the PTC thermal performance and hence on the net output power generation so it increases the overall efficiency of the system. Therminol VP-1 power plant using 5% Al_2O_3 Nano annual efficiency is found to be 16.06%; whereas Therminol VP-1 and 5% Cu Nano particles has 16.11% of annual solar to electric efficiency. Solar salt power plant using 5% Al_2O_3 Nano particles has 17.03% solar to electric efficiency; whereas solar salt using 5% Cu Nano particles has 17.18% overall annual efficiency which is 6.2% higher than the pure solar salt case.

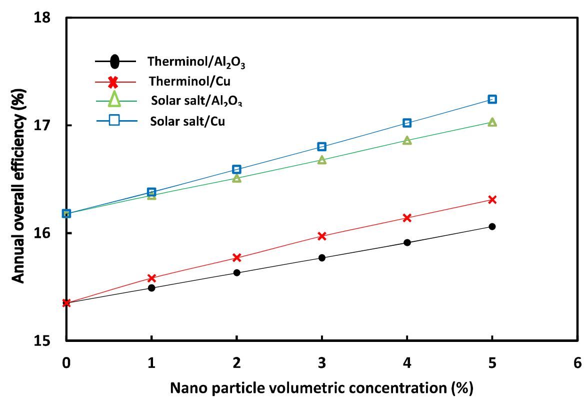

FIGURE 6. Annual electric-to-solar efficiency for Therminol VP-1 and solar salt Nano fluids

Based on the results discussed in sections (3.1) and (3.2) the best case scenario is found to be using solar salt as a HTF and 5% of Cu Nano particles. Using wind energy generation system is found to produce 1.56 GWh of additional power based on the Meteorological data of the location and only within the available PTC field area using the proposed wind turbine regardless the CSP-Wind ratio of the location. The hybrid system is applied on the basis of best case scenario among the investigated cases. The Simulation results show that wind energy has energy sharing percentage about 1.5% of the hybrid CSP-Wind-Nano model field as simplified in Fig. (7).

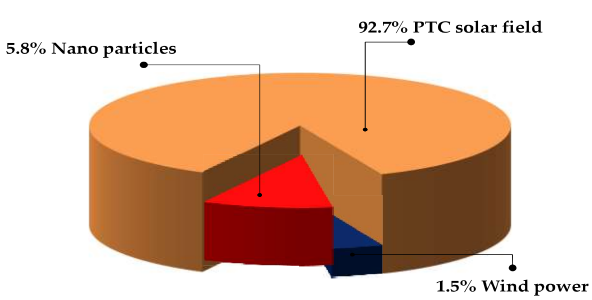

FIGURE 7. Hybrid CSP-Wind energy generation using solar salt and 5% Cu Nano particle concentration

3.3 Monthly performance simulation results

Monthly performance simulation process is divided into two steps. First step is carried out to estimate the net wind energy for the proposed wind turbine model. The wind power generation, throughout a complete year based on the monthly average wind speed, is shown in the following Fig. (8). Maximum monthly wind generation is found to be about 260 MWh in April since wind speed is in its peak value in this month in New Capital location according to Meteonorm 7.0 [29] data base.

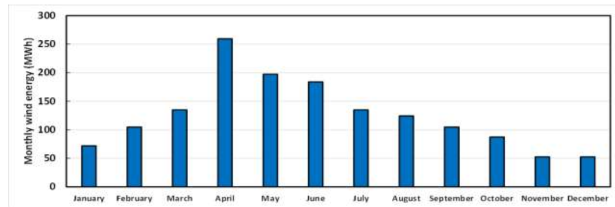

FIGURE 8. Monthly wind power generation for New Capital location

The second step of the simulation is carried out for the investigated solar power plant using both HTF and different concentrations of Nano particles for the meteorological data of the New Capital of Egypt. Results show that the maximum monthly produced solar energy occurs during July since it possesses the maximum DNI. Fig. (9) and (10) show the monthly output solar energy using Therminol VP-1 and Al_2O_3 and Cu Nano particles respectively. During July pure Therminol VP-1 power plant produces 9.81 GWh. Similar to the simulation results in annual performance the Cu Nano particles are found to have better enhancement on the PTC thermal performance and hence on the net output solar energy generation. During July Therminol VP-1 power plant using 5% Al_2O_3 Nano particles is found to produce 10.2 GWh; whereas Therminol VP-1 and 5% Cu Nano particles produces 10.32 GWh of solar energy as shown in Fig. (10). The least values of DNI are found to be in January and hence the corresponding output solar energy is found to decrease to be about 57% of its maximum value during July. Fig. (11) and (12) show the monthly output solar energy using solar salt as a HTF and Al_2O_3 and Cu Nano particles respectively. During July pure solar salt power plant produces 10.16 GWh. During July solar salt power plant using 5% Al_2O_3 Nano particles is found to produce 10.62 GWh; whereas Therminol VP-1 and 5% Cu Nano particles produces 10.83 GWh of solar energy as shown in Fig. (11) and (12) respectively.

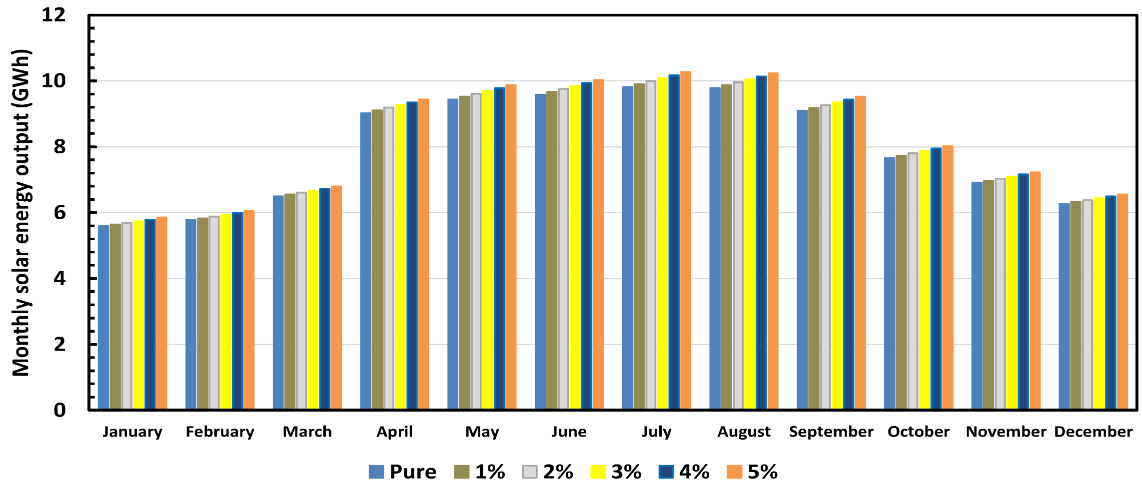

FIGURE 9. Therminol VP-1 and Al_2O_3 Nano particles monthly produced solar energy

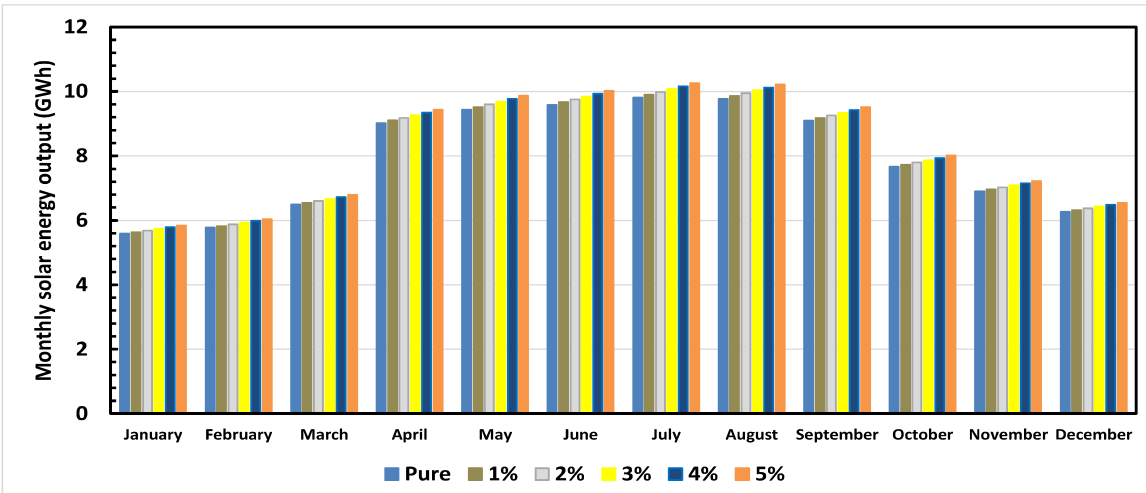

FIGURE 10. Therminol VP-1 and Cu Nano particles monthly produced solar energy

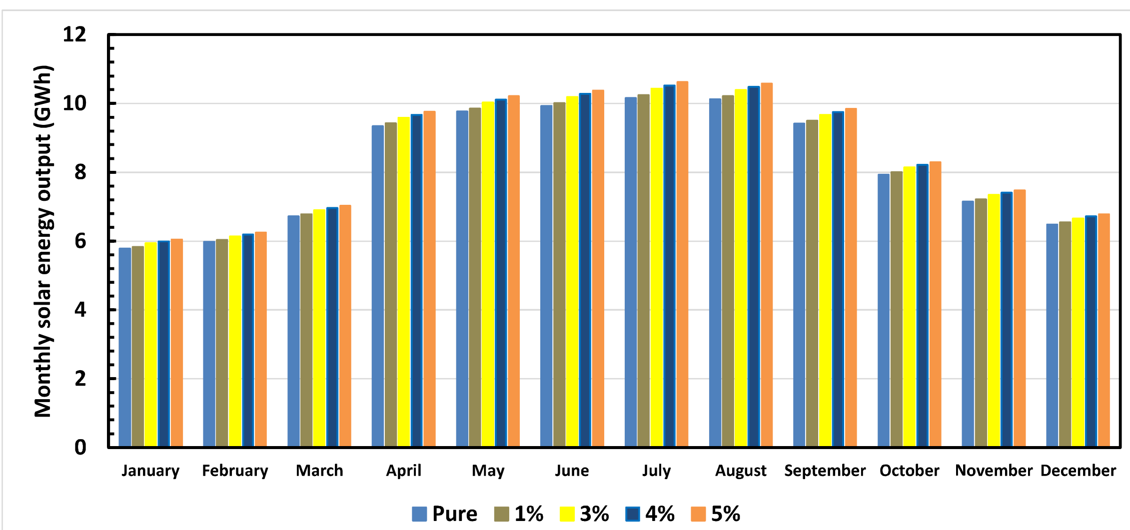

FIGURE 11. Solar salt and Al_2O_3 Nano particles monthly produced solar energy

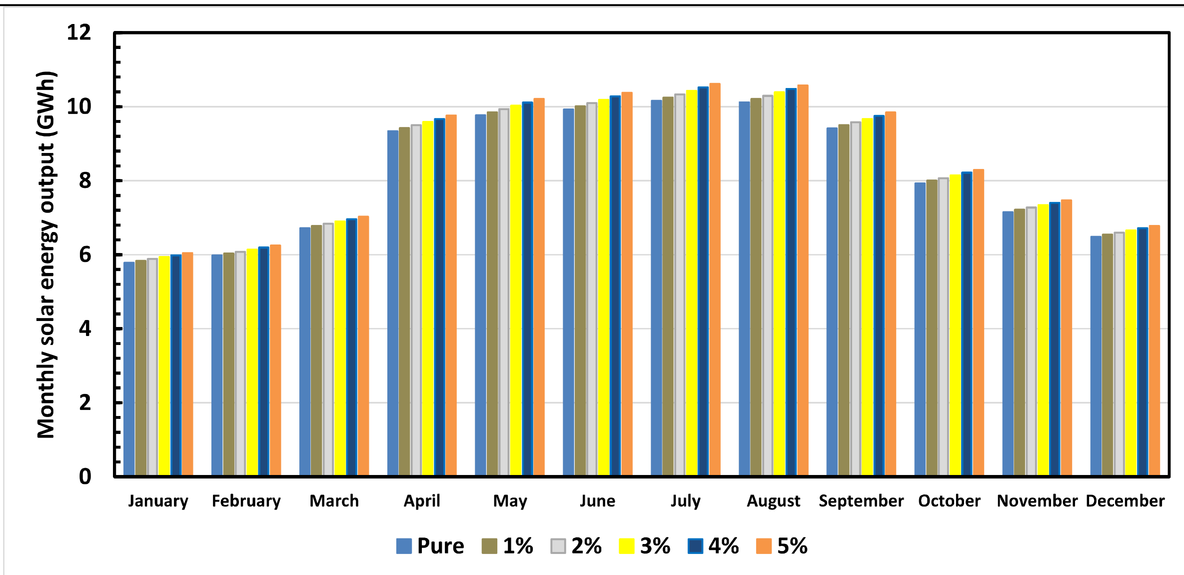

FIGURE 12. Solar salt and Cu Nano particles monthly produced solar energy

To elaborate the differences between monthly solar output energy profiles shown in Fig. (8), (9), (10) and (11) the results of pure Therminol VP-1 and solar salts using 5% of Al_2O_3 and Cu Nano particles are summarized and combined in the following Fig. (13). The investigated location of New Capital of Egypt has the maximum and minimum values of monthly DNI in July and January respectively and hence the corresponding maximum and minimum output solar energy generation are in July and January as well.

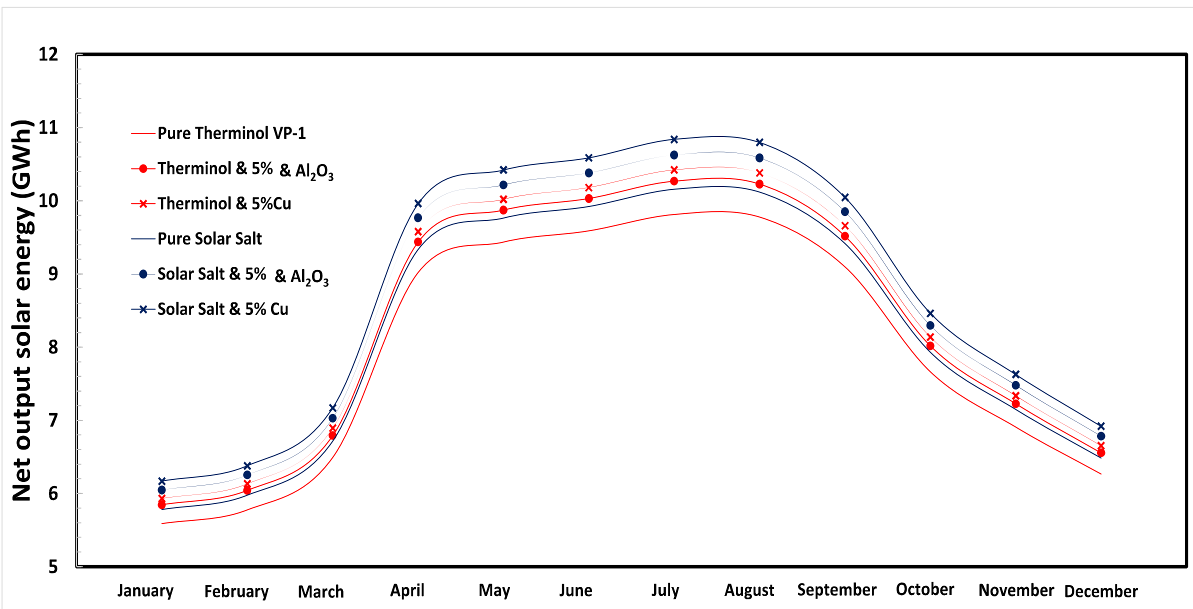

FIGURE 13. Monthly output solar energy for both HTF using 5% concentration of both Nano particles

4. Conclusions

- This study investigates the hybrid solar-wind power generation for the meteorological data of New Capital of Egypt location. The present work proposes a PTC solar power plant based on a real implemented power plant design using two different HTF with different concentrations of Al_2O_3 and Cu Nano particles. The best investigated case is found to be solar salt as a HTF and 5% of Cu Nano particles.
- The main conclusion of this study is that Nano particles have significant effect on the thermo-physical properties of the HTF and therefore they may have significant influence over the solar power plant performance.
- Using Nano particles additives with the solar field HTF improves the thermal performance of the HTF but Cu Nano particles are found to give better thermal performance compared to Al_2O_3 Nano particles.
- Solar salt as a HTF is a promising solar field fluid but it has a very high freezing point which is the main drawback for its operation during the non-DNI and cloudy operational times. Solar salt can replace the conventional types of HTF for PTC applications since it can work under specifically

higher temperature ranges which enhances the steam production process for Rankine cycle.

- Results indicate that the wind power generation would add about 1.5% increase in the net power generation for the wind-solar hybrid system using the proposed wind turbine model; whereas Nano particles additives would add up to 5.8 % increase in the net output power regardless the wind to CSP ratio of the proposed location.
- Solar salt as a HTF using 5% of Cu Nano particles gives the best performance among the investigated cases for the steady state conditions regardless the fluctuations of DNI, transient operational conditions and the night time operation.

References:

[1] IPCC. Climate change synthesis Report, 2007.

[2] UN climate change conference Paris 2015.

[3] R.P.P., Abdul Baseer, M., Awan, A.B., Zubair, M, Performance Analysis and optimization of a parabolic Trough solar power plant in the Middle East Region, Energies (2018). **11** .741.

[4] K.M. Powell, K. Rashid, K. Ellingwood, J. Tuttle, B. D. Iverson, Hybrid concentrated solar thermal power systems. Renewable and Sustainable Energy Reviews (2017). **80**. 215–237.

[5] M.D.A. Al-Falahi, S.D.G. Jayasinghe, H. Enshaei, A review on recent size optimization methodologies for Stand-alone solar and wind hybrid renewable energy systems, Energy conversion Management, (2017). **143**. 252–274.

[6] S.S. Dihrab and K. Sopian, Electricity generation of hybrid PV/Wind System in Iraq, Renewable Energy, (2010). **35**. 1303–1307.

[7] S. Ravelli, G. Franchini, A. Perdichizzi, S. Rinaldi, and V. E. Valcarenghi, Modeling of Direct Steam Generation in Concentrating Solar power, Energy Procedia, (2016). **101**. 464–471.

[8] M. Biencinto, M. J. Montes, L. Valenzuela, L. Gonzalez, Simulation and comparison between fixed and Sliding pressure strategies in parabolic trough solar power plants with direct steam generation. Applied thermal Engineering, (2017). **125**. 735–745.

[9] E.M. Zarza, A. Giglio, A. Lanzini, P. Leone, M. M. R. Garcia, Direct steam generation in parabolic trough collectors, Renewable and Sustainable Energy Reviews, (2017). **74**. 453–473.

[10] J. F. Feldhoff, M. Eickhoff, L. Keller, J. L. Alonso, M. M. Grünefeldt, L. Valenzuela, J. Perpeintner, T. Hirsch, Status and first results of the DUKE project, Energy procedia, (2014). **49**. 1766–1776.

[11] Sokrates project DLR-AP1&2, SOKRATES-Projekt Solarthermische Kraftwerkstechnologie für den Schutz des Erdklimas, Institute of Solar Research, (2004).

[12] I.L. Garcia, J.L. Alvarez and D. Blanco, Performance model for parabolic trough solar thermal power plants with thermal storage: Comparison to operating plant data, Solar Energy, (2011). **85**. 2443–2460.

[13] Y. Li, Y. Yang, Impacts of solar multiples on the performance of integrated solar combined cycle systems with two direct steam generation fields, Applied Energy, (2015). **160**. 673–680.

[14] W. Al-Maliki, F. Alobiad, V. Kez, B. Epple, Modelling and dynamic simulation of a parabolic trough power plant, Journal of process control, (2016). **39**. 123–138.

[15] L. Salgado C., A. Rodrignez, G. Calderón, Thermal performance of parabolic trough solar collectors, Renewable and Sustainable Energy Reviews, (2017). **67**. 1345–1359

[16] S. A. Kalogirou, A detailed thermal model of a parabolic trough collector receiver, Energy, (2012). **48**. 298–306.

[17] E. Bellos, C. Tzivanidis and K.A. Antonopoulos, A detailed working fluid investigation for solar parabolic trough collectors
, Applied Thermal engineering (2017). **114**. 374–386.

[18] Z. D. Cheng, Y. L. He, F. Q. Cui, R. J. Xu, Y. B. Tao. Numerical simulation of a parabolic trough solar collector with non-uniform solar flux. Solar Energy. 2012, **86**, 1770–1784.

[19] D. Bishoyi, K. Sudhakar, Modelling and performance simulation of 100 MW PTC based solar thermal power plant in Udaipur India, Case studies in Thermal Engineering, (2017). **10**. 216–226.

[20] G. Colangelo, E. Favale, A. Risi, D. Laforgia, Results of experimental investigation on the heat conductivity of Nano-fluid based on diathermy oil for high temperature applications, Applied Energy, (2012). **97**. 828–833.

[21] A. Kasaeian, S. Daviran, R. D. Azarian, A. Rashidi, Performance evaluation and nano-fluid using capability study of a solar parabolic trough collector, Energy conversion and Management, (2015). **89**. 368–375.

[22] V. Ferraro, J. Settino, M. A. Cucumo, D. Kaliakastos, Parabolic trough system operating with Nano-fluid, Energy procedia, (2016). **101**. 782–789.

[23] E. Bellos and T. Christos, Parametric investigation of nanofluids utilization in parabolic trough Collectors, Thermal Science and Engineering process, (2017). **2**. 71–79.

[24] X. Li, Chan. Zou, L. Zhou, A. Qi, experimental Study on the thermal-physical properties of diathermic oil based SiC Nano-fluids for high temperature applications, International Journal of Heat and Mass Transfer, (2016). **97**. 631–637.

[25] National Renewable Energy Laboratory [NREL], Nevada Solar-One project.

[26] A. Giostri, M. Binotti, M. Astolfi, P. Silva, E. Macchi and G. Manzolini, Comparison of different solar plants based on parabolic trough technology, Solar Energy, (2012). **86**. 1208–1221.

[27] National Renewable Energy Laboratory [NREL], Archimede project.

[28] Technical Data Sheet, Therminol VP-1 Heat Transfer Fluid

[29] https://www.meteonorm.com/

[30] T. Sokhansefat, A. Kasaeian, F. Kowsary, Heat transfer enhancement in parabolic trough collector tube using Al2O3/synthetic oil Nano fluid, Renewable Sustain Energy Reviews, (2014). **33**. 636–644.

[31] T. Miller, T. Zinkle, B. Chin, Strength and fatigue of dispersion-strengthened copper, Journal of Nuclear Materials (1991). 179. **181**. 263–266.

[32] Siemens SST 700/900 Economical dual casing steam turbine for Reheat applications.

[33] A. Giostri, C. Saccilotto, P. Silva, E. Macchi, G. Manzolini, A Numerical model for off design performance calculation of parabolic trough based solar power plant, 4th Proceeding L ASME, (2010).

[34] H. Zang, M. Wang, J.Huang, W. Zhinong, S.G. Guoqiang, A Hybrid Method for Generation of Typical Meteorological Years for Different Climates of China, Energies, (2016). **9**. 12.

[35] M. Biencinto, L. Gonzalez, E. Zarza, Performance model and annual yield comparison of parabolic trough solar thermal power plants with either Nitrogen or Synthetic oil as heat transfer fluid, Energy conversion and managements, (2014). **87**. 238–249.

[36] T.A Stuetzle, Automatic control of the 30 MWe SEGS VI parabolic trough plant, Master thesis, University of Wisconsin, (2002).

[37] R.S. Lopez, J. Fradera, S.C. Lopez, Molten salts database for energy applications, Chemical Engineering and Processing, Process Intensification, (2013). **73**. 82–102.

[38] M. Genc , M. A. Ezan, A. Turgut, Thermal performance of a nanofluid-based flat plate solar collector: A transient numerical study, Applied Thermal Engineering, (2018). **130**. 395–407.

[39] R.S. Vajjha , D.K. Das, A review and Analysis influence of temperature and concentration of Nano-fluids on thermo physical properties, heat transfer and pumping power, International Journal of Heat and Mass Transfer, (2012). **55**. 2063–2078.

[40] S.G Han, M.W. Park, I.K.Yu, Real time simulation scheme for stand –alone wind power generation, IFAC power plants and power systems control. (2003). **36**. 20.

[41] C. Carrillo, A.F.O. Montano, J. Cidras, E.D. Dorado, Review of power curve modeling for wind turbines, Renewable and sustainable, Energy Reviews, (2013). **21**. 572–581.